Submitted to: *The Journal of Drug Targeting*

Green Fluorescent Protein (GFP): is seeing believing and is that enough?

Susan A. Shorter, Marie W. Pettit, Paul D. R. Dyer, J. Emma Coakley-Youngs, Monique A.M. Gorringe-Pattrick, Samer El-Daher and Simon C. W. Richardson[1*]

IDS Laboratory, Department of Life and Sports Science, Faculty of Engineering and Science, University of Greenwich, Central Avenue, Chatham Maritime, Kent, ME4 4TB.

Correspondence should be addressed to: Dr Simon Richardson

Tel: +44(0) 208 331 8207

Fax: +44(0) 208 331 9805

Email: S.C.W.Richardson@Greenwich.ac.uk

Green Fluorescent Protein: is seeing believing and is that enough?

Abstract:

Intracellular compartmentalisation is a significant barrier to the successful nucleocytosolic delivery of biologics. The endocytic system has been shown to be responsible for compartmentalisation, providing an entry point, and trigger(s) for the activation of drug delivery systems. Consequently, many of the technologies used to understand endocytosis have found utility within the field of drug delivery. The use of fluorescent proteins as markers denoting compartmentalisation within the endocytic system has become commonplace. Several of the limitations associated with the use of green fluorescent protein (GFP) within the context of drug delivery have been explored here by asking a series of related questions: (1) Are molecules that regulate fusion to a specific compartment (*i.e.* Rab- or SNARE-GFP fusions) a good choice of marker for that compartment? (2) How reliable was GFP-marker overexpression when used to define a given endocytic compartment? (3) Can glutathione-s-transferase (GST) fused in frame with GFP (GST-GFP) act as a fluid phase endocytic probe? (4) Was GFP fluorescence a robust indicator of (GFP) protein integrity? This study concluded that there are many appropriate and useful applications for GFP; however, thought and an understanding of the biological and physicochemical character of these markers are required for the generation of meaningful data.

Key words: GFP, marker, endocytosis, protein stability, protease, drug delivery, membrane.

Author Contributions: SCWR conceived, found funding for, supervised this work and wrote the manuscript. MWP, SAS and PD performed the protein biochemistry experiments, MG-P, EC-Y and SE-D and SCWR performed the overexpression experiments.

List of Abbreviations: Bovine Serum Albumin (BSA), Early Endosomal Antigen 1 (EEA1), Enhanced Green Fluorescent Protein (eGFP), Glutathione-s-transferase (GST), Lysosome Associated Membrane Protein (LAMP), Phosphate Buffered Saline (PBS), Rat Sarcoma (Ras)-related in brain (Rab), Texas Red labelled (TxR)- Wheat-germ agglutinin (WGA) (TxR-WGA).

Disclosure statement: The authors report no conflicts of interest.

Introduction.

The scientific method requires the iterative gathering and interpretation of evidence used to test a hypothesis (Wagensberg, 2014). The careful design of experiments helps mitigate the possibility of the misinterpretation of data and is, consequently, something deserving of a great deal of attention. Reliable interpretation requires an understanding of the tools used during an empirical investigation, and this paper seeks to further characterise some of the uses (and missuses) of Green Fluorescent Protein (GFP), a tool that has had a profound impact upon the world of cell biology, within the context of drug delivery and gene therapy (Wahlfors *et al.,* 2001).

GFP and its fluorescent variants (Wachter, 2006) have been widely used since the discovery that a mutation of residue 65 (from serine to threonine), dramatically improved its spectral properties (Heim *et al.,* 1995). GFP is commonly used as a protein "tag" that has been readily visualised in fixed or live cells either directly, using its intrinsic fluorescence *i.e.* "Brainbow" technology (Weissman and Pan, 2015), or indirectly using antibodies which have been identified via a secondary antibody conjugated to a fluorophore, radioisotope or enzyme (Nakamura *et al.,* 2008). Here a further investigation into the usefulness of GFP within the context of drug delivery has been undertaken. Four questions pertinent to the use of GFP within various experimental situations have been posed: (1) Are molecules that regulate fusion to a specific compartment (*i.e.* Rab- or SNARE- GFP fusion proteins) a good choice of marker for that compartment (compartments described in figure 1)? (2) How reliable were GFP-marker overexpression experiments when used to define a given endocytic compartment? (3) Can GST-GFP act as a fluid phase endocytic probe? (4) Was GFP fluorescence a robust indicator of (GFP) protein integrity?

Materials and Methods.

Equipment: The orbital shaker, French Press, centrifuges (RC6 Plus) and microtiter plate reader (Microplate Photometer Multiskan FC) were from ThermoFischer, (Loughbourgh, UK). The mini-PROTEAN tetra cell, minitrans-blot, electrophoretic transfer cell and power supplies were from BioRad (Hemel Hempstead, UK). Fluorescence spectra were measured using a Fluoromax- 4 spectrofluorometer (Horiba Scientific, Middlesex, UK). Microscopic images were obtained using either: an Eclipse 90i microscope (Nikon UK Ltd., Surrey, UK) fitted with an Apo60 objective and a DS-Qi1Mc camera or an inverted Zeiss LSM880 fitted with a plan apochromat 63x (numerical aperture 1.40) oil emersion objective, (Carl Zeiss Ltd., Cambridge, UK) both with dedicated software. *GST-GFP production and enrichment:* The production and enrichment of glutathione-s-transferase (GST) fused in frame with GFP (GFP-GST) has been previously described (Pettit *et al.*, 2014). In brief *Escherichia coli* MC1061 were transformed with pGFP-GST [GenBank JN232535.1] and were cultured in 10mL of 2xYT (containing 25 µg/mL ampicillin) overnight at 37 ^{o}C shaking at 200 RPM. This culture was used to inoculate 1000 mL of 2xYT (containing 25 µg/mL ampicillin), which was left to incubate for 4 hours at 37 ^{o}C shaking at 200 rpm prior to the addition of IPTG to a final concentration of 1 mM. After an additional 4 h incubation, the bacteria were sedimented by centrifugation (6 000 xG for 10 min., at 4 ^{o}C). The bacterial pellet was suspended in 10 mL of PBS containing 10x EDTA free COmplete^{TM} protease inhibitor cocktail (Roche, Burgess Hill, UK). The bacterial suspension was then subject to lysis using a French Press set to 1500 psi to avoid the possibility of recombinant protein conformational relaxation (associated with detergent lysis). Sodium azide (final concentration of 0.02 % (w/v)) was then added to the preparation as a bacteriostatic. The GST-GFP protein was then enriched by affinity chromatography using glutathione-conjugated Sepharose 4b (GE Healthcare, Bucks, UK), in accordance with the manufacturer's instructions and characterised

using gel electrophoresis, Coomassie staining and Western immunoblotting. *Spectroscopic and fluorescence analysis of GST-GFP*. Previously spectrophotometric characterisation of GST-GFP determined that a wavelength of 484 nm was optimal for GFP excitation and was in agreement with the literature (Pettit *et al.,* 2014). Consequently, GST-GFP emission spectra were recorded using an excitation wavelength of 484 nm using a Fluoromax- 4 spectrofluorometer (Horiba Scientific, Middlesex, UK). *GST-GFP stability and pull-down experiments*: Enriched GST-GFP (500 μg) (in PBS) was placed in a sterile Eppendorf tube. Where a pull-down experiment was performed, glutathione conjugated Sepharose 4b beads (GE Healthcare, Bucks, UK) (200 μl bed volume in PBS) were added to the tube. The specified amount of protease was added to each tube and incubated at 37 ^{o}C for the specified time. When performing pull-down experiments the preparation was subject to sedimentation (1 min., at 14 000 rpm 4^{o} C) and the emission spectra, or emission at 492 nm, for the supernatant was measured as stated. The pellet was suspended in 1 mL of PBS. Finally, 10 μl of this was then added to 1 mL of Laemmli buffer for analysis Western immunoblotting using a GFP specific polyclonal antibody (Cat No. CAB4211; Invitrogen, Paisley, UK). The emission spectra of the supernatants (after excitation at 484 nm) were recorded, prior to the addition of the Laemmli buffer. *Cell culture, microscopy and "pulse-chase" experiments*: Vero cells (ATCC number CCL-81), were cultured as previously described (Dyer *et al.,* 2015). Purified GST-GFP in PBS was filter sterilised using a 0.2 micron filter (Milipore Ltd, Hertfordshire, UK) and added to cultured cells at a concentration of 1 mg/mL in the presence of 200 μM Leupeptin (Sigma-Aldrich Company Ltd., Dorset, UK). This "pulse" of GST-GFP was added to complete cell culture media and incubated for 4 hours at 37 ^{o}C. The cells were then washed three times with fresh sterile PBS and returned to incubate in complete media for an additional 20h at 37^{o}C in 5% (v/v) CO_2. The cells were then washed 3 times in PBS and fixed with either cold methanol or formaldehyde (as noted) and as previously described (Dyer

et al., 2013; Dyer *et al.*, 2015). Immunostaining was performed as previously described (Richardson *et al.*, 2004; Richardson *et al.*, 2008; Dyer *et al.*, 2013; Dyer *et al.*, 2015) using EEA1 (BD Bioscience,) LAMP1 or LAMP2 specific monoclonal antibodies (DHSB hybridoma bank, University of Iowa, USA) as previously described (Richardson *et al.*, 2004; Richardson *et al.*, 2008; Dyer *et al.*, 2015). *Over-expression experiments:* were conducted as previously described (Richardson *et al.*, 2004). Briefly, $5x10^5$ Vero cells / well were used to seed a 6 well plate. To each well, complete media was added to a final volume of 1.5 mL and the plate placed in a humidified cell culture incubator (37 ^oC; 5% (v/v) CO_2) overnight. *Pulse-chase and transfection experiments.* Texas Red labelled (TxR)-wheat-germ agglutinin (WGA) (TxR-WGA) (Invitrogen, Paisley, UK), was used at a concentration of 10 µg/mL in complete media containing 200 µM leupeptin (Sigma Chemical Company, Dorset, UK). Cells were incubated with TxR-WGA for 4 hours and then transfected using lipofection over 4 hours and incubated for a further 40 hours prior to fixation. Lipofection was performed using Lipofectamine 2000 (Invitrogen, Paisley, UK) as per the manufacturer's instructions using 2.5 µg of plasmid per well. The eGFP-Rab5 encoding plasmid has been previously described (Richardson *et al.*, 2004; Roberts *et al.*, 1999). Where there was no transfection cells were subject to a pulse (4 hours), washed 3 times with PBS and then incubated for a further 20 hours in complete media prior to fixation. *Sequence comparisons;* were performed using the DNAStar software suite by Lasergene (Madison WI, USA). Protein sequences were obtained (http://www.uniprot.org) and analysed using the MegaAlign application (DNAStar by LASERGENE, Madison WI) deploying the Clustal-W algorithm. Protein sequence identities (and UniProt reference numbers) are given (table 1).

Results.

Sequence comparisons as an indicator of marker viability. When the primary protein sequences of the Rat Sarcoma (Ras)-related in brain (Rab)5 isoforms a, b and c were analysed, a very high level of sequence identity was evident (table 2, *i.e.* between 81.9 and 87.4 %). Given the antigens used to generate the selection of antibodies to Rab5 documented (table 3), it was unlikely that the antibodies listed would be specific for a given isoform, given the identity (%) between the antigens used to raise them. The similarity between the various primary protein sequences of isoforms of the Rab6-subfamily (Rab6a, Rab6a', Rab6b, Rab6c and Rab41) was also striking (table 4, *i.e.* between 98.6 – 61.3% sequence identity). Table 5 describes the antigens used to raise selective commercially available antibodies and further emphasises the capacity for mislabelling specific isoforms of Rab6 using commercially available antibodies. Table 6 describes the levels of protein sequence similarity that result from comparing syntaxin7 and syntaxin12 (also called syntaxin13), which also demonstrated a high level of sequence identity (56.2%).

Over-expressed GFP-fusion proteins as intracellular markers. In an effort to evaluate the compartmentalisation of transiently expressed eGFP-Rab5a in relation to an endocytosed probe (TxR-WGA), eGFP-Rab5a was expressed in Vero cells. EEA1 has been well documented as a Rab5 binding partner (Simonsen *et al.,* 1998), which interacts with membrane inositol phosphates (Simonsen *et al.,* 1998). Figure 2 (panels: (a) (anti-EEA1 localisation), (b) (eGFP-Rab5a) and (c) (merge) show a considerable degree of co-localisation, with specific examples of vesicles positive for both EEA1 and eGFP-Rab5a being denoted by arrows in the inset. These vesicles are of a size, distribution and morphology typical of Vero cells (Dyer *et al.*, 2013; Richardson *et al*., 2008; Richardson *et al*., 2004). Figure 2 also shows the effect of probing cells expressing eGFP-Rab5a (panel d) with TxR-WGA (panels e). The expanded vesicular structures positive for both TxR-WGA

and eGFP-Rab5a (panel f) were profound. This phenotype has been associated with very high (~50 µg/mL) concentrations of WGA (Dyer *et al.*, 2013) or the constitutively active, GTP locked Rab5 mutant, Rab5:Q79L (Barbieri *et al*., 1996). Figure 2 (panel g) shows cells that have been incubated with TxR-WGA after transient transfection with eGFP-Rab5:Q79L (panel i). The similarity in phenotype (*i.e.* expanded GFP positive vesicles) between eGFP-Rab5a co-incubated with WGA (panel e) and the eGFP-Rab5:Q79L mutant (panel h) was striking. Figure 2 (panel i) shows the co-localisation of TxR-WGA and the overexpressed eGFP-Rab5:Q79L mutant. In the absence of the Rab5 transfection TxR-WGA (panel j) can be seen localising to a LAMP1 positive (late endocytic) compartment (panel l). Specific examples of vesicles positive for both TxR-WGA and LAMP1 have been denoted by arrows (inset).

GFP fluorescence as a marker for protein integrity. Figure 3 (panel a) shows the emission spectra of GST-GFP over time and there was no readily quantifiable alteration in emission spectra over the 300min documented. The protease trypsin (~0.5units / 500µg GST-GFP) also had very little effect upon the emission spectra of GST-GFP over 300min (panel b), which was similar to the effect produced by adding proteinase k (10units / 500µg GST-GFP) (panel c). When the integrity of the protein GST-GFP was examined by Western immunoblotting, it was evident that at 5min, both trypsin (~0.5 units / 500µg GST-GFP) and proteinase k (10 units / 500µg GST-GFP) had digested GST-GFP, whereas the negative control (no protease) was stable over 300min. A solution to this impasse *i.e.* using the spectral properties of GFP to monitor protein integrity, was found by using the GST portion of GST-GFP to bind to glutathione-conjugated Sepharose after protease treatment and, after washing away any non-bound material, assaying for fluorescence emission at 492 nm (figure 3: panel e).

The use of GFP as an endocytic probe. The utility of eGFP as a probe for endocytic capture (*i.e.* as cargo) was explored (figure 4). The late endocytic marker lysosome associated

membrane protein (LAMP)1 has been well-characterised and localises to late endosomes, endolysosomes and lysosomes (Chen *et al.*, 1985). The anti-LAMP1 and anti-LAMP2 antibodies required the fixation of cells in cold methanol for immunofluorescence work. After MeOH fixation, little GFP signal was evident (figure 4: panel a) despite the LAMP1 signal being readily detectable (panel b). After fixation using aldehyde, the signal from GST-GFP (panel d) was clearly coincident with that from TxR-bovine serum albumin (BSA) (panel e), which, at 24h, has been reported resident in a late endocytic compartment (panel f) (Richardson *et al.*, 2008). The data describing the localisation of GST-GFP relative to TxR-BSA (panels d, e and f) appears to be substantiated by those describing the location of GST-GFP (panel g) relative to early endosomal marker EEA1 (panel h) after 24h. Here there appears to be some signal from GFP, however, there was some, but not exclusive localisation between GFP-GST and EEA1. Figure 4 (panel j) highlights another problem with using GFP-GST as a probe. Here, aldehyde fixed cells co-labelled with TxR-WGA, display a marked lack of GFP signal (panel j) relative to a robust TxR-WGA signal (panel k) when examined using an LSM880. This made assessing the level of co-localisation very difficult (panel l).

Discussion.

When interpreting data from single cell assays, a variety of assumptions are often made with regard to the nature of a GFP “tag". The first is that if the GFP molecule has been degraded, then fluorescence output would be reduced accordingly. The second is that a GFP tagged molecule will behave in a way that was representative of the analogue it was being used to mimic. Finally, there remains an assumption that because a molecule has been documented in a specific location, that location is where the molecule in question must function. This final observation is a fallacy, as a molecule will be observed where there is a large pool of the molecule, even a reservoir, which may not necessarily be the place where the molecule functions. However, unpacking this assumption is beyond the scope of this paper. The first and second assumptions are challenged herein by addressing the questions stated in the introduction:

Are molecules that regulate fusion to a specific compartment (i.e. Rab- or SNARE-GFP fusions) a good choice of marker for that compartment? The various Rab5 isoforms documented (table 2) generally have the same intracellular distribution (*i.e.* to early endocytic compartments) (Chen *et al.*, 2014). Consequently, the issue of misidentifying a Rab5 isoform would not present a huge problem in terms of mislabelling a specific intracellular compartment. Most intracellular markers occupy more than one intracellular compartment, a specific example being the transferrin receptor, which is often used as a marker for recycling endosomes (*i.e.* a Rab11 enriched compartment) (Richardson, 2010). This receptor cycles through early and recycling endosomes *en route* to the plasma membrane, and back to the early endosome after internalisation. The Rab6 subfamily of proteins is a little more diverse than the various isoforms of Rab5, regulating fusion through the Golgi network (Liu and Storrie, 2015). However, specific isoforms have demonstrated tissue specific expression. Rab6b has been found mainly in neuronal cells (Opdam *et al.*, 2000), and Rab6c has been

documented in: brain, testes, prostate and breast tissue (Young *et al.*, 2010). Functional variance between Rab6a and Rab6a' has been reported during the retrograde transport of ricin (Utskarpen *et al*., 2006; Liu and Storrie, 2015). Consequently, the result of mislabelling a particular Rab6 isoform, or expressing it in an inappropriate cell type, may be a little more misleading. The result of misidentifying syntaxin proteins, such as 7 and 13, may be more drastic as misidentifying them would, in all likelihood, lead to the generation of false positives or negative conclusions in relation to subcellular distribution or trafficking. Syntaxin13 typically catalyses vesicle fusion events between early endocytic structures, such as early endosomes (McBride *et al.*, 1999). Syntaxin7, also a t-soluble *N*-ethylmaleimide sensitive factor attachment protein receptor (SNARE) heavy chain, catalyses both heterotypic and homotypic fusion to late endosomes (Mullock *et al.*, 2000; Pryor *et al.*, 2004). The similarity between the protein sequences of all of these molecules makes the generation of specific polyclonal antibodies challenging. The consequences of misidentifying syntaxin7 and 13 have been reported (Mullock *et al.*, 2000). Here additional immunodepletive steps to removed cross-reactive antibodies were taken to ensure antibody specificity (Mullock *et al.*, 2000).

Equivalently, monoclonal antibodies may be used to identify molecules that act as compartmental "doorkeepers", responsible for regulating fusion to, and consequently the identity of a specific intracellular compartment (Dyer *et al.*, 2013). This is considerably more time consuming and expensive than generating polyclonal antisera. Given the challenges and expense associated with generating polyclonal or monoclonal antibodies, specific for proteins with such a high degree of similarity, it may be easier and more accurate to express these molecules as GFP-fusion proteins. Rather than immunodetecting Rab6a and Rab6a' after siRNA knockdown, qPCR has been used (Utskarpen *et al*., 2006). This approach has many limitations with regard to examining the trafficking of endocytosed cargo within the context

of single-cell assays, but is certainly worth considering when using a population based cell assay. When considering the utility of a specific marker, the general and the specific need to be considered separately, given that there are nearly always exceptions to any rules of thumb. An example might be the distribution of syntaxin6 in melanocytes. In B16F10 cells syntaxin6 has been documented to localise to late endosomes (Wade *et al.*, 2001). However, this localisation has been reported to be melanocyte specific and would not be expected in more generic epithelial cells.

How reliable were GFP-marker overexpression experiments when used to define a given endocytic compartment? Over a 24h timeframe, a pulse of WGA has been documented in a late endocytic compartment, which would normally contain markers including LAMP1 (or 2), lysosomal hydrolases (such as cathepsin D), or even well-characterised probes such as bovine serum albumin (BSA) or BSA-colloidal gold, subject to endolysosomal translocation (Mullock *et al.,* 2000). The dose of WGA (typically from 5-50 µg/mL) may also impact upon the morphology of late-endocytic compartments, however, here the dose of TxR-WGA was kept constant at 10 µg/mL as previously this had given a robust signal at a minimal concentration (of WGA) (Dyer *et al.,* 2013). Observing a profound co-localisation between overexpressed eGFP-Rab5a and WGA at 48h post-transfection was unexpected (figure 2: panels d-f), as previously, at this time, the internalised WGA and Rab5 might be expected to occupy late and early endocytic compartments respectively (Dyer *et al.,* 2013). This confusion was further underscored by the localisation of eGFP-Rab5 to an early endosomal antigen (EEA)1 positive compartment (figure 2: panels a-c). Moreover, after 24h, WGA was recorded in a LAMP positive set of vesicular structures (figure 2: panels j, k and l). These data are further contradicted by previously published data reporting eGFP-Rab5a localising to EEA1positive structures that are typically early endocytic (*i.e.* on early endosomes) (Simonsen *et al.,* 1998; Roberts *et al.,* 1999), yet WGA, when chased into eGFP-Rab5a

overexpressing cells can be seen in dramatically expanded Rab5 positive structures (figure 2: panels d-f). Given that EEA1 not only interacts with the Rab protein, as an effector, but also inositol phosphates on the early endosomal membrane (Simonsen *et al.,* 1998), it is unlikely (although still possible), that the EEA1 signal was simply being redistributed by the overexpressed eGFP-Rab5a. Further, there are examples of Rab5a overexpression being separate and discreet from late endocytic markers (Dyer *et al.,* 2013). Confusion was compounded by the data describing the eGFP-Rab5:Q79L mutant, a GTP locked constitutively active mutant of Rab5 (Barbieri *et al.,* 1996). This has been documented to cause expanded vesicles that have often lost their compartmental identity as the "doorkeeper" or Rab protein regulating fusion becomes hyperactive (Barbieri *et al.,* 1996). It is possible that the cells documented (panels d, e and f) were expressing a lot of Rab5a, which gave rise to a phenotype similar to that of the Rab5:Q79L mutant. Equivalently the phenotype observed may be due to an interaction between the WGA and the effects of Rab5 overexpression. This may not impact upon the assumption that the GFP tagged protein will behave in a similar way to its wild type analogue as this variance in phenotype may not be due to any alteration in protein function, but is instead due to there being much more Rab5 than would normally be found in a healthy cell. It is important to note that when using these tools, in these specific circumstances, a degree of compartment identity has been lost. Care should also be exercised when using algorithms to quantitate the degree of co-localisation. Commonly used methods to quantify co-localisation include the use of Pearson's correlation coefficient (adapted by Manders) that are quite subjective though maybe useful if applied appropriately (Richardson *et al.,* 2004; Dunn *et al.,* 2011). Their usefulness is also defined by the definition of co-localisation being employed and the inferences being made. If these experiments are an attempt to discover the function of a specific protein and are attempting to resolve individual molecules, they may also be limited by the resolution of even super-resolution techniques

(Dunn *et al.,* 2011). Figure 2 (panels j, k and l) clearly show late endocytic markers partitioned into microdomains, contained within the same vesicle. However, as there are varying degrees of co-localisation at the level of the pixel, as opposed to the vesicle, false negatives may result.

Was GFP fluorescence a robust indicator of (GFP) protein integrity? GFP stability in the presence of proteases has been reported to be high (Aoki *et al.,* 2008). Here the authors used a binding assay similar to the "pulldown" assay described here (figure 3: panel e) to monitor protein integrity (Aoki *et al.,* 2008). Figure 3 (panels a-d) documents the effects of both proteinase k and trypsin upon the fluorescence of eGFP. Previously GST-GFP was sequenced using mass spectrometry, and determined both its absorption and emission spectra in relation to eGFP determined (Pettit *et al.,* 2014). GST-GFP was found to exhibit maximum excitation when stimulated at 484nm with an emission peak at 492nm. This was in contrast to eGFP, which displays a maximum excitation peak at 488nm and an emission peak at 509nm (Pollock and Heim, 1999). When either protease was used to digest GST-GFP (confirmed by Western immunoblotting (figure 3: panel d), the fluorescence spectra remained unaltered after digestion (figure 3: panels a-c). The simplest explanation for the apparent disconnect between fluorescence and GST-GFP molecular weight, was that the fluorophore located within the eGFP beta-barrel spanning helix remained partially intact after digestion. This was unexpected. However, practically, this particular phenomenon was relatively easy to circumvent if the GFP molecule was designed to contain an affinity "tag" to aid enrichment. An example might be a 6-histidine tag or a GST "tag" as documented here (figure 3: panel e).

Can GST-GFP act as a fluid phase endocytic probe? Given the well-characterised effects of pH upon eGFP's fluorescent properties (Roberts *et al.,* 2016) it was not surprising to note the aberrant compartmentalisation of GST-GFP post-endocytic capture. Very recently, the problem of eGFP's instability at low pH has been addressed using tandem dimer GFP

variant (Ishil *et al.,* 2007; Roberts *et al.,* 2016), however the problem of lysosomal proteases and methanol fixation remain. For optimal fluorescence yield, eGFP has been reported to require aldehyde fixation rather than fixation in cold methanol (Dyer *et al.,* 2013). Consequently, the combination of low pH, methanol fixation and the presence of lysosomal proteases would not predispose eGFP as a robust fluid phase endolysosomal marker. This was underscored in figure 4. Consequently, it may be more advantageous to use a transiently or stably expressed, well-characterised fluorescent protein fused to the cytosolic termini of a lysosomal trans-membrane protein as a marker such as LAMP1-RFP (Sherer *et al.,* 2003). Finally, the choice of marker should also be dictated by application. Is it essential to know how many molecules are in a given compartment for optimal therapeutic effect? If so then perhaps a radiolabel is a more useful "tag" than any fluorescent molecule due to the ease of quantification. Previously, we have published a study quantifying the modulation of subcellular distribution mediated by of a series of well-defined radiolabelled poly(amidoamine) polymers after their administration *in vivo* (Richardson *et al.,* 2010). When the possibility of optimising a dose to minimise non-specific side effects is considered, the use of radioprobes remains attractive. That said radioprobes have limited use relative to fluorescent probes within the context of a single cell assay, which is also very useful for early stage evaluation of advanced drug delivery system function and subcellular distribution (Seib, *et al.,* 2006; Richardson *et al.,* 2008).

Conclusion.

GFP remains a useful tool to evaluate subcellular trafficking, providing the limitations associated with its biochemistry are understood. This is true of any marker used to define a compartment. GFP's stability and fluorescent properties are not intimately connected, consequently care needs to be taken when designing experiments that might expose GFP to proteases either during *in vitro* cell free assays or in a cell based assay. These observations highlight some of the pitfalls working with eGFP. More generally, they also highlight the need for carefully designed experiments, a need to understand and characterise the tools you are using and the use of multiple controls in order to interrupt the data they produce in a useful and meaningful way. Is seeing believing? No, though clearly fluorescent proteins are extremely useful tools though as ever, context is everything.

References.

Aoki T., Tsuchida S., Yahara T., Hamaue N. (2008), Novel assays for proteases using green fluorescent protein-tagged substrate immobilized on a membrane disk. *Anal. Biochem.*, **378**(2):132-7. doi: 10.1016/j.ab.2008.04.022.

Barbieri M. A., Li G., Mayorga L. S., Stahl P. D. (1996) Characterization of Rab5:Q79L-Stimulated Endosome Fusion, *Archives of Biochemistry and Biophysics*, **326** (1):64-72, doi: 10.1006/abbi.1996.0047.

Chen J.W., Murphy T.L., Willingham M.C., Pastan I., August J.T. (1985), Identification of two lysosomal membrane glycoproteins, *J. Cell Biol.*, **101**(1):85-95.

Chen P.I., Schauer K., Kong C., Harding A.R., Goud B., and Stahl P.D. (2014), Rab5 isoforms orchestrate a "division of labor" in the endocytic network; Rab5C modulates Rac-mediated cell motility, *PLoS One*, **9**(2):e90384. doi: 10.1371/journal.pone.0090384.

Dyer P.D., Shepherd T.R., Gollings A.S., Shorter S.A., Gorringe-Pattrick M.A., Tang C.K., Cattoz B.N., Baillie L., Griffiths P.C., Richardson S.C. (2015), Disarmed anthrax toxin delivers antisense oligonucleotides and siRNA with high efficiency and low toxicity. *J. Control Release*, **220**(Pt A):316-28. doi: 10.1016/j.jconrel.2015.10.054.

Dyer P.D., Kotha A.K., Pettit M.W., Richardson S.C. (2013), Imaging select mammalian organelles using fluorescent microscopy: application to drug delivery, *Methods Mol Biol.* **991**:195-209. doi: 10.1007/978-1-62703-336-7_19.

Dunn K. W., Kamocka M. M. and McDonald J. H. (2011), A practical guide to evaluating colocalization in biological microscopy, Am. J. Physiol. Cell Physiol., 300(4): C723–C742, doi: 10.1152/ajpcell.00462.2010.

Heim R., Cubitt A. B. and Tsien R. Y. (1995), Improved green fluorescence, Nature, 373 (6516); 663-4. doi:10.1038/373663b0.

Ishii M., Kunimura J.S., Jeng H.T., Penna T.C., Cholewa O. (2007), Evaluation of the pH- and thermal stability of the recombinant green fluorescent protein (GFP) in the presence of sodium chloride. *Appl Biochem Biotechnol*., **137-140**(1-12):555-71. doi: 10.1007/s12010-007-9079-6.

Liu S., and Storrie B. (2015), How Do Rab Proteins Determine Golgi Structure? *Int. Rev. Cell Mol. Biol*., **315**:1–22. doi:10.1016/bs.ircmb.2014.12.002.

McBride, H.M., Rybin, V., Murphy, C., Giner, A., Teasdale, R., and Zerial, M. (1999), Oligomeric complexes link Rab5 effectors with NSF and drive membrane fusion via interactions between EEA1 and syntaxin 13. *Cell*, **98**: 377–386.

Mullock B. M., Smith C. W., Ihrke G., Bright N. A., Lindsay M., Parkinson E. J., Brooks D. A., Parton R. G., James D. E., Luzio J. P., Piper R. C. (2000), Syntaxin 7 Is Localized to Late Endosome Compartments, Associates with Vamp 8, and Is Required for Late Endosome–Lysosome Fusion. *Mol. Biol. Cell.*, **11**: 3137–3153.

Nakamura K.C., Kameda H., Koshimizu Y., Yanagawa Y., Kaneko T. (2014), Production and histological application of affinity-purified antibodies to heat-denatured green fluorescent protein, *J. Histochem Cytochem.,* **56(**7):647-57. doi: 10.1369/jhc.2008.950915.

Opdam F.J., Echard A., Croes H.J., van den Hurk J.A., van de Vorstenbosch R.A., Ginsel L.A., Goud B., Fransen J.A. (2000), The small GTPase Rab6B, a novel Rab6 subfamily member, is cell-type specifically expressed and localised to the Golgi apparatus. *J. Cell Sci.* **113**(15):2725–2735.

Pettit M.W., Dyer P.D., Mitchell J.C., Griffiths P.C., Alexander B., Cattoz B., Heenan R.K., King S.M., Schweins R., Pullen F., Wicks S.R., Richardson SC. (2014), Construction and physiochemical characterisation of a multi-composite, potential oral vaccine delivery system (VDS), *Int. J. Pharm.,* **468**(1-2): 264-71. doi: 10.1016/j.ijpharm.2014.03.046.

Pollok B. A. and Heim R. (1999), Using GFP in FRET-based applications, *Trends in Cell Biology*, **9**(2):57-60.

Pryor P. R., Mullock B. M., Bright N A., Lindsay M. R., Gray S. R., Richardson S. C. W., Stewart A., James D. E., Piper R. C., & Luzio J. P. (2004), Combinatorial SNARE complexes with VAMP7 or VAMP8 define different late endocytic fusion events, *EMBO reports*, **5**(6):590-595.

Richardson S. C. W. (2010), Tracking Intracellular Polymer Localization Via Fluorescence Microscopy, in: *Organelle-Speci c Pharmaceutical Nanotechnology*, Edited by Volkmar Weissig and Gerard G. M. D'Souza P117-193.

Richardson S.C., Wallom K.L., Ferguson E.L., Deacon S.P., Davies M.W., Powell A.J., Piper R.C., Duncan R. (2008), The use of fluorescence microscopy to define polymer localisation to the late endocytic compartments in cells that are targets for drug delivery, *J. Control. Release*, **127**(1):1-11. doi: 10.1016/j.jconrel.2007.12.015.

Richardson S.C., Pattrick N.G., Lavignac N., Ferruti P., Duncan R. (2010) Intracellular fate of bioresponsive poly(amidoamine)s *in vitro* and *in vivo*. *J. Control. Release*, **142**(1):78-88. doi: 10.1016/j.jconrel.2009.09.025.

Richardson S.C., Winistorfer S.C., Poupon V., Luzio J.P., Piper R.C. (2004), Mammalian late vacuole protein sorting orthologues participate in early endosomal fusion and interact with the cytoskeleton, *Mol Biol Cell.,* **15(**3):1197-210.

Roberts R. L., Barbieri M. A., Pryse K.M., Chua M., Morisaki J.H., Stahl P.D. (1999) Endosome fusion in living cells overexpressing GFP-rab5. *J. Cell Sci.,* **112** (21): 3667-75.

Roberts T.M., Rudolf F., Meyer A., Pellaux R., Whitehead E., Panke S., Held M. (2016), Identification and Characterisation of a pH-stable GFP, *Scientific Reports* **6**, Article number: 28166, doi:10.1038/srep28166.

Seib P. F., Jones A., Duncan R. (2007), Comparison of the endocytic properties of linear and branched PEIs, and cationic PAMAM dendrimers in B16f10 melanoma cells, J. Controlled Release, 117(3):291-300, DOI: 10.1016/j.jconrel.2006.10.020.

Simonsen A., Lippe R., Christoforidis S., Gaullier J-M., Brech A., Callaghan J., Toh B-H., Murphy C., Zerial M. & Stenmark H. (1998) EEA1 links PI(3)K function to Rab5 regulation of endosome fusion *Nature* **394**, 494-498. doi:10.1038/28879.

Sherer N.M., Lehmann M.J., Jimenez-Soto L.F., Ingmundson A., Horner S.M., Cicchetti G., Allen P.G., Pypaert M., Cunningham J.M., Mothes W. (2003) Visualization of retroviral replication in living cells reveals budding into multivesicular bodies, *Traffic,* **4**(11):785-801

Utskarpen A., Slagsvold H. H., Iversen T-G., Walchli S., and Sandvig K., (2006) Transport of Ricin from Endosomes to the Golgi Apparatus is Regulated by Rab6A and Rab6A'. *Traffic*, **7**: 663–672 doi: 10.1111/j.1600-0854.2006.00418.x.

Wachter R.M., (2006), The family of GFP-like proteins: structure, function, photophysics and biosensor applications. Introduction and perspective, *Photochem Photobiol.* **82**(2): 339-44.

Wade N., Bryant N. J., Connolly L. M.,, Simpson R. J., Luzio J. P., Piper R. C., and James D. E. (2001) Syntaxin 7 Complexes with Mouse Vps10p Tail Interactor 1b, Syntaxin 6, Vesicle-associated Membrane Protein (VAMP)8, and VAMP7 in B16 Melanoma Cells. *JBC*, **276**(23):19820–19827, DOI 10.1074/jbc.M010838200.

Wagensberg J. (2014) On the Existence and Uniqueness of the Scientific Method, *Biol Theory*, **9**(3): 331–346, doi: 10.1007/s13752-014-0166-y.

Wahlfors J., Loimas S., Pasanen T., Hakkarainen T. (2001), Green fluorescent protein (GFP) fusion constructs in gene therapy research, *Histochem Cell Biol.*, **115**(1): 59-65.

Weissman T.A., Pan Y.A. (2008), Brainbow: new resources and emerging biological applications for multicolor genetic labeling and analysis. *Genetics*. **199**(2) :293-306, doi: 10.1534/genetics.114.172510.

Young J, Ménétrey J, Goud B. (2010), RAB6C is a retrogene that encodes a centrosomal protein involved in cell cycle progression. *J. Mol Biol*., **397**(1): 69–88.

Acknowledgements.

All of the authors, particularly SCWR would like to acknowledge Ruth Duncan's mentoring over the years in both CPT and within the IDS laboratory. SAS, MG-P, EC-Y and MWP would like to thank the Faculty of Engineering and Science, University of Greenwich for funding their PhD studies.

Tables.

Table 1: Protein sequence identity. Adapted from: Echard *et al*., 2001, Liu and Storrie 2015 and the Uniprot (www.uniprot.org) and Abcam (www.abcam.com) websites.

Protein	UniProt reference	Antibody (AbCam)	Comment
Rab5a	P20339	ab18211, polyclonal CT from aa150	Required for: fusion to the plasma membranes (exosome release) and early endosomes, the maturation of apoptotic cell-containing phagosomes and filopodia extension. Two isoforms.
Rab5b	P61020	ab72907, polyclonal (CT aa150 onwards)	Two isoforms, probably increases Rab5 activity during fusion to the early endosome
Rab5c	P51148	ab209475, monoclonal, (proprietary antigen)	Two isoforms, probably increases Rba5 activity during fusion to the early endosome
Rab6a	P20340	Ab95954 polyclonal (aa 1 -178)	Golgi ribbon organisation
Rab6a'	No entry	No entry	Ubiquitously expressed, similar to Rab6, overexpression of a constitutively active mutant inhibits the secretory pathway, though doesn't redistribute Golgi proteins to the ER. Utilizes a different set of effectors relative to rab6a (Echard et al., 2000).
Rab6b	Q9NRW1	Ab206110 (aa 31-193)	Retrograde membrane traffic at the level of the Golgi complex, Intra-Golgi vesicle transport. Selectively expressed in neuronal cells.
Rab6c	Q9H0N0	ab113838 (aa 118-167)	Retrograde transport Endosome to Golgi and Golgi to ER, Intra-Golgi transport. Only expressed in brain, testis, prostate, and breast tissue.
Rab41	Q5JT25	Ab201305 (aa 124-169)	Two isoforms differing at amino acid 42. Not found in liver. Retrograde endosome to Golgi transport, intra-Golgi transport. Retrograde Golgi to ER transport
Syntaxin7	O15400	ab152867, (aa 1-261)	Mediates late endosomal homotypic and late endosomes to lysosome heterotypic vesicular fusion (Mullock *et al.,* 2000).
Syntaxin12 (aka Synt13)	Q86Y82	Ab13261 (aa 1-276)	Mediates and regulates fusion to early endosomes (Mullock *et al.,* 2000).

Table 2: Rab5 family members and their level of protein sequence identity. Rab5a isoform 2 is identical to isoform 1 with the exception of the deletion of "AAFLTQTVCLDDTT" in isoform 2. Rab5b isoform 2 is identical to isoform 1 with the exception of the deletion of "TFARAKTWVKELQRQASPSIVIALAGNKADLANKRMVEYEE" in isoform 2. Rab5c isoform 2 contains an additional N-terminal "MELSWRSPSPLSASLHSTSPHPHALWTTTAGRA". In each instance isoform 1 has been used in the above.

	Identity (%)			
Divergence (%)		Rab5a	Rab5b	Rab5c
	Rab5a	-	87.4	84.7
	Rab5b	13.8	-	81.9
	Rab5c	17.2	20.8	-

Table 3: Antigen similarity (identity (%) for select Rab5-specific antibodies (listed in table 1)

Identity (%)	Rab5a	Rab5b	Rab5c
Polyclonal Rab5 antibody	100	72.3	76.9
Polyclonal Rab5b antibody	72.3	100	76.9

Table 4: Rab6-subfamily members and their level of protein sequence identity

	Identity (%)	Rab6a	Rab6a'	Rab6b	Rab6c	Rab41
Divergence (%)	Rab6a	-	98.6	90.9	89.9	66.7
	Rab6a'	1.5	-	91.3	89.4	65.7
	Rab6b	9.8	11.4	-	82.2	61.3
	Rab6c	10.9	20.4	20.4	-	67.6
	Rab41	43.9	45.7	54.0	42.2	-

Table 5: Antigen similarity (identity (%) for Select Rab6 subfamily-specific antibodies

Identity (%)	Rab6a	Rab6b	Rab6c	Rab41
Polyclonal Rab6a antibody	-	93.9	88.0	63.0
Polyclonal Rab6b antibody	93.9	-	76.0	58.7
Polyclonal Rab6c antibody	88.0	76.0	-	55.9
Polyclonal Rab41 antibody	63.0	58.7	55.9	-

Table 6: Similarity (identity (%)) between the primary structure of syntaxin7 and 12 (13)

	Identity (%)		
Divergence (%)	-	Syntaxin 7	Syntaxin 12
	Syntaxin 7	-	56.2
	Syntaxin 12	64.7	-

Figures.

Figure 1: Cartoon Depicting Select Markers Defining Endocytosis and Exocytosis. This cartoon depicts both the endocytic and exocytic trafficking pathways and some of the more commonly used markers to identify organelles therein. Summarised are the various probes that have been documented within specific compartments over time. Adapted from (Mullock *et al.*, 2001; Richardson *et al.*, 2008; Dyer *et al.*, 2013)

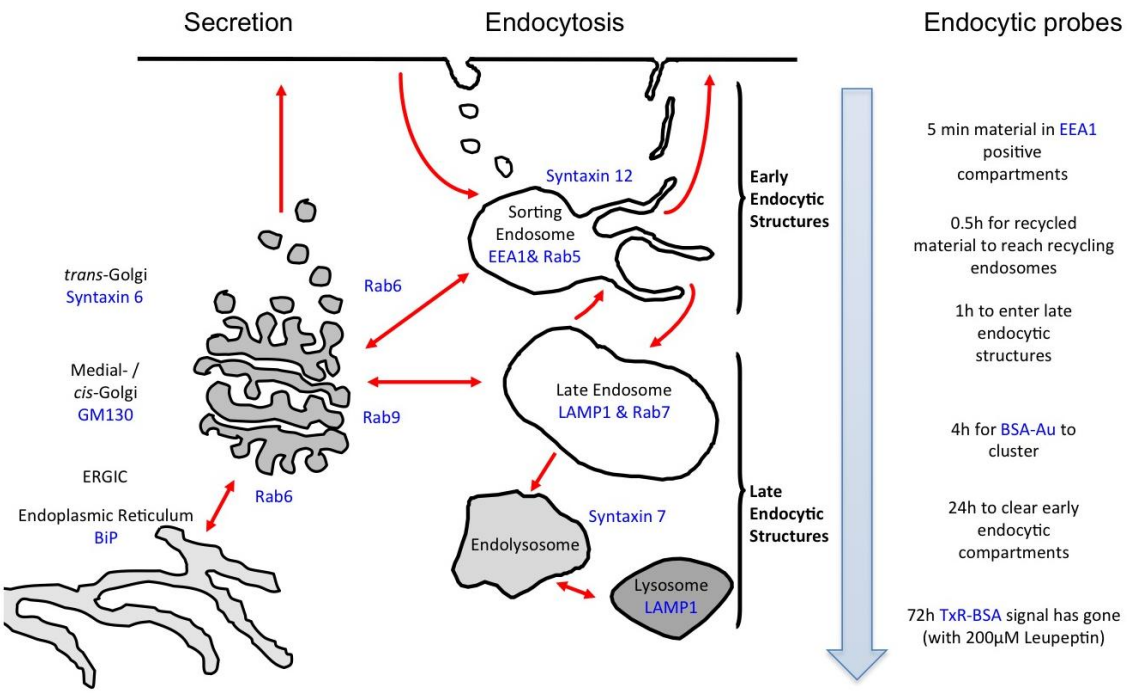

Figure 2: Aberrant eGFP-Rab5a compartmentalisation and vesicular morphology. Here (panels a, b & c), eGFP-Rab5a transiently transfected Vero cells were aldehyde fixed and immunolabelled with a monoclonal anti-EEA primary antibody and a TxR conjugated- anti mouse secondary antibody 48 hours after transfection using Lipofectamine 2000. Panel (a) shows the detection of an anti-EEA1 antibody, panel (b) shows the eGFP signal and panel (c) is a merge of the red and green channel. Co-localisation was evident and exemplified by arrows in the panels inset (panels a & b). Panels (d, e and f) record Vero cells also transiently transfected with eGFP-Rab5a that have also been exposed to TxR-WGA (10µg/mL for 4h at 37ºC) and then chased for an additional 40h in complete media containing 200µM leupeptin also at 37ºC. Panel (d) depicts the red channel, panel (e) documents the green channel and panel (f) is a merge of the red and green channels. Panels (g, h & i) show Vero cells transiently transfected with eGFP-Rab5:Q79L and fed TxR-WGA as above after 48h. Panels (j, k and l) depict Vero cells incubated with TxR-WGA as above, and fixed in cold methanol before being immunolabelled with monoclonal primary antibody specific for LAMP2. This antibody was then detected using a mouse–IgG specific AlexaFluor 488 conjugated secondary. Imaging was on a Zeiss LSM880.The size bar is equal to approximately 5 microns.

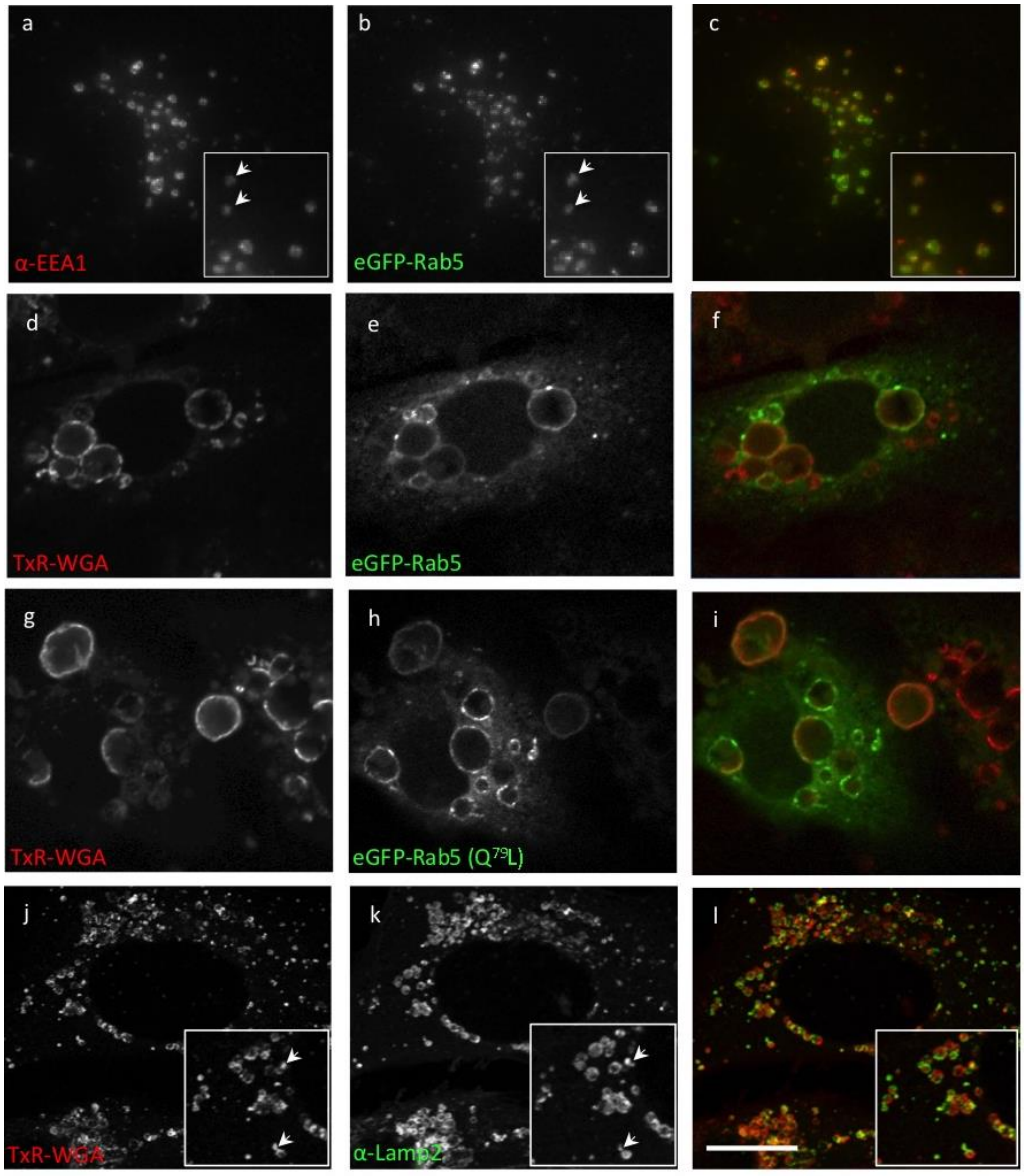

Figure 3: GFP Fluorescence and Stability in Relation to Protease Activity. Panel (a) documents the emission spectra of GST-GFP over 300 min in PBS after excitation at 484nm. The emission spectra of GST-GFP after exposure to ~0.5 units / 500µg GST-GFP of trypsin is shown (panel b) also over a similar time frame. Panel (c) documents the emission spectra of GST-GFP after exposure to 10units / 500µg GST-GFP of proteinase k. Panel (d) explores the molecular weight of GST-GFP by Western immunoblotting after 300min in PBS, 5 and 10min exposure to either 10units / 500µg GST-GFP, of proteinase k or ~0.5 units / 500µg GST-GFP of trypsin. Panel (e) documents the ability to affinity isolate GST-GFP from a protease digestion and then use the GFP portion of GST-GFP to quantify protein integrity using GST-GFP's emission at 492nm.

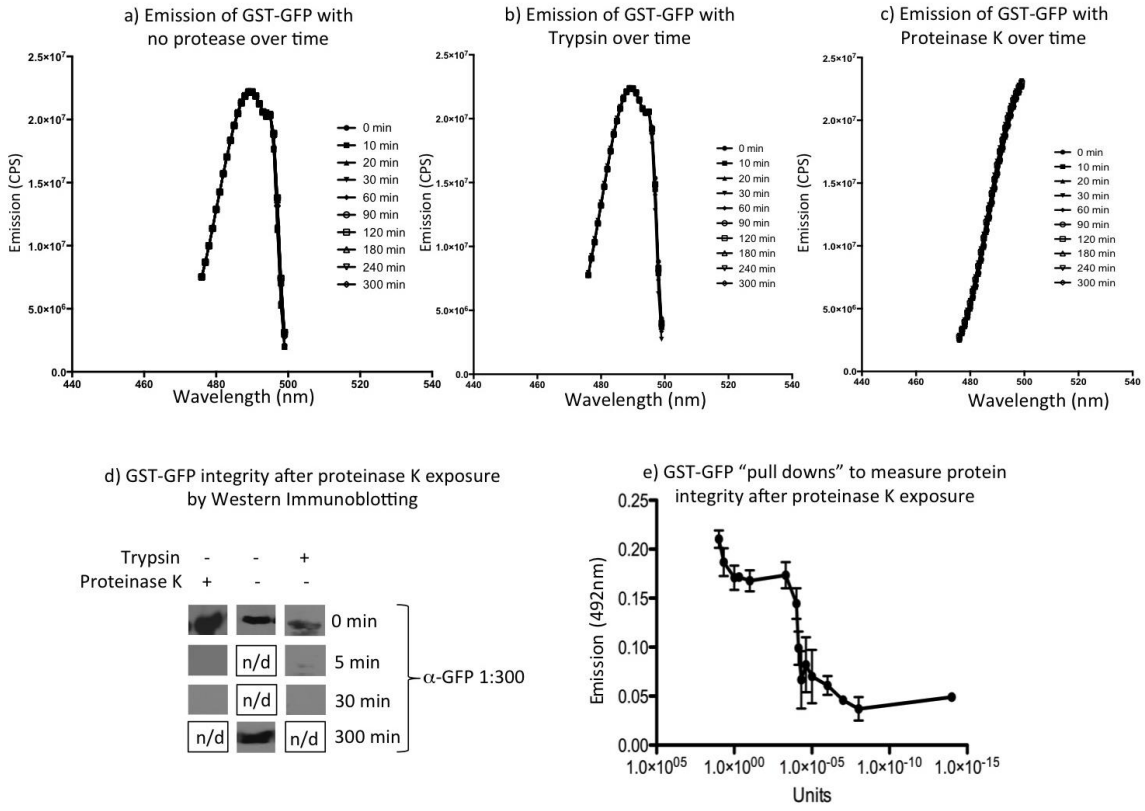

Figure 4: Use of GFP as an endocytic probe. Panels (a, b and c) document Vero cells fixed in methanol, 20h after a 4h pulse of GST-GFP in complete media with 200µM leupeptin. These cells were then immunostained using an anti-LAMP1 monoclonal antibody and a mouse IgG specific – TxR conjugated secondary antibody. Aldehyde fixed cells (panels d, e and f) fixed 20h after a 4h pulse with both GST-GFP and TxR-BSA were documented. The localisation of a GST-GFP pulsed (as described above) to a compartment labelled with a primary monoclonal antibody specific for EEA1 and a mouse specific TxR labelled- secondary is documented (panel: (g) (GST-GFP), (h) (anti-EEA1) and (i) (merge). These micrographs were acquired using a Nikon Ti-20 microscope. The localisation of GST-GFP, pulsed and chased as before is documented (panels j, k and l). The signal from GST-GFP (panel j) is very weak; where as the signal from a pulse of TxR-WGA (panel k) is robust. A merge (panels j and k) is shown and these images were acquired using a Zeiss LSM880. The size bar represents approximately 5 microns.